IEEE Access
Multidisciplinary ⋮ Rapid Review ⋮ Open Access Journal

Received March 27, 2021, accepted April 5, 2021, date of publication April 9, 2021, date of current version April 19, 2021.

Digital Object Identifier 10.1109/ACCESS.2021.3072134

Design of a Dual-Mode Graphene-on-Microring Resonator for Optical Gas Sensing

JIAQI WANG[1], XINYING ZHANG[1], ZHIWEI WEI[1], HUABIN QIU[1], YUZHI CHEN[1], YOUFU GENG[1], YU DU[1], ZHENZHOU CHENG[2,3], (Senior Member, IEEE), AND XUEJIN LI[1]

[1]Shenzhen Key Laboratory of Sensor Technology, College of Physics and Optoelectronic Engineering, Shenzhen University, Shenzhen 518060, China
[2]School of Precision Instruments and Optoelectronics Engineering, Tianjin University, Tianjin 300072, China
[3]Key Laboratory of Opto-electronic Information Technology, Ministry of Education, Tianjin 300072, China

Corresponding authors: Youfu Geng (gengyf@szu.edu.cn) and Zhenzhou Cheng (zhenzhoucheng@tju.edu.cn)

This work was supported in part by the National Natural Science Foundation of China under Grant 61805164, Grant 61805175, and Grant 61775149; in part by the Science and Technology Plan Project of Shenzhen under Grant JCYJ20190808120801661 and Grant JCYJ20190808145207437; in part by the Foundation of Key Laboratory of Opto-electronic Information Technology, Ministry of Education, Tianjin University, Tianjin, China, under Grant 2020KFKT008; and in part by the Teaching Reform Research Project of Shenzhen University under Grant JG2019068.

ABSTRACT On-chip optical gas sensors, which use resonant shifts of cavities to detect molecular concentrations, have the advantages of high sensitivity, real-time detection, and compact footprint. However, such sensors are usually limited by a serious cross-sensitivity issue induced by environmental temperature variations. To overcome this limitation, we study a dual-mode graphene-on-microring resonator to accurately measure gas concentrations without suffering from temperature variations. To be specific, the influences of gas-induced graphene's optical conductivity changes and environmental temperature variations on effective refractive indices of TE_0 and TE_1 modes in the resonator can be decoupled based on the modal linear independent responses. With this method, we designed a nitrogen dioxide sensor with a sensitivity of 0.02 nm/ppm and a limit of detection of 0.5 ppm. Our study paves the way for developing on-chip optical gas sensors with excellent sensitivity and temperature stability.

INDEX TERMS Silicon photonics, graphene, optical gas sensing, integrated optics, multimode waveguide.

I. INTRODUCTION

Compact and low-cost gas sensors have wide applications in consumer electronics, industrial safety, medical diagnosis, environmental monitoring, vehicle exhaust measurement, and public security. To date, different types of gas sensors have been demonstrated, such as electrochemical gas sensors [1], semiconductor gas sensors [2], [3], and optical gas sensors [4]–[7]. Among these sensors, optical gas sensors, namely, fiber sensors [8], [9], surface plasmon resonance sensors [10], [11], and waveguide-integrated sensors [12], [13], have the advantages of high sensitivity, fast response, and electromagnetic immunity [14]. Taking advantage of state-of-the-art CMOS technology, silicon-based waveguide-integrated sensors are most promising to be integrated with optoelectronic and electronic devices for achieving monolithically chip-integrated sensing, signal processing, and communication [15]. Therefore, they have attracted great attention in the past decades.

On the other hand, graphene is an intriguing material to develop optical gas sensors [16]. Adsorbed gas molecules act as charge-carrier donors or acceptors to change graphene's optical conductivity, which leads to phase or intensity changes of photonic devices. Moreover, by integrating graphene on a waveguide, the graphene sheet can interact with light in the waveguide through the evanescent field coupling [17], [18], significantly elongating the light-molecules interaction length. As a result, optical gas sensors based on graphene-covered photonic integrated circuits (PICs) have been a hot research topic. Based on this platform, researchers have developed structures, such as electrically gated graphene-on-silicon nanowires [19], graphene-on-germanium slot waveguides [20], and graphene-on-silicon microring resonators (MRRs)[21] for the trace gas detection.

Moreover, with the advantages of high sensitivity, fast response, and label-free detection, refractive index (RI) sensors have been widely demonstrated for gas sensing. In such

The associate editor coordinating the review of this manuscript and approving it for publication was Maged Abdullah Esmail.

devices, gas molecules in the ambient environment alternate the RI of a waveguide, resulting in a phase change of the optical mode. Then, the phase change can be detected by measuring wavelength shifts via micro-cavities, dispersive devices, or interference structures. For example, K. Li *et al.* demonstrated a RI gas sensor based on a silicon photonic crystal microcavity which is composed of a silicon slab triangular photonic crystal with a few holes replaced by a slot [22]. M. Singh *et al.* studied a dual-band stop vertical hybrid plasmonic filter based on a silicon nitride fin Bragg grating for methane sensing [23]. R. Shamy *et al.* designed a mid-infrared on-chip Mach-Zehnder interferometer gas sensor based on a suspended silicon waveguide [24]. However, the temperature variation condition is commonly present in industrial RI sensing applications. Several works have proposed methods to solve this issue based on microwave sensors for the liquid RI sensing, such as using a reference mode to compensate for the temperature change [25] and developing an artificial neural network model to restore the sensor's response to the material under test regardless of the varying temperature [26]. It is necessary to develop a method to eliminate the influence of the temperature variation for the RI gas sensor.

In this paper, we studied a dual-mode graphene-on-MRR RI gas sensor to overcome the cross-sensitivity problem. We theoretically analyzed the influences of gas-induced graphene's optical conductivity changes and environmental temperature variations on effective RIs of the TE_0 and TE_1 modes in the graphene-on-MRR. Our study shows that graphene and temperature-induced RI variations can be extracted separately due to the modal linear independent responses to these two factors. Based on this model, we designed a nitrogen dioxide (NO_2) gas sensor with a sensitivity of 0.02 nm/ppm and a limit of detection (LOD) of 0.5 ppm. Our study paves the way for developing sensitive on-chip optical gas sensors without suffering from temperature fluctuations.

II. SENSING PRINCIPLE OF THE DUAL-MODE GRAPHENE-ON-MRR

First, the influence of the gas doping on graphene's Fermi level (E_x) can be expressed as follows [16],

$$E_x = \hbar V_F \sqrt{\frac{4\pi(\Delta n + n_i)}{g_\upsilon g_s}}, \tag{1}$$

where V_F is the Fermi velocity, $g_v = g_s = 2$ are the valley degeneracy and the spin degeneracy, respectively. n_i is the graphene's initial carrier concentration (before gas doping). Δn is the change of the graphene's carrier concentration due to the gas doping. As for NO_2 molecules, Δn can be given by the following empirical formula [16],

$$\Delta n = (-0.18247 + 5.59596 C_{NO_2} + 0.04481 C_{NO_2}^2) \times 10^{10}, \tag{2}$$

where C_{NO2}(ppm) is the concentration of NO_2. Besides, due to the selectivity of the gas adsorption, the change of the Fermi level of graphene is related to gas species [16]. Therefore, the selective responses of graphene optical gas sensors could be used for sensing multiple gas molecules.

Second, based on the graphene's Fermi level, the optical conductivity (σ) of graphene can be calculated by Kubo formula [27],

$$\begin{aligned}\sigma = &-\frac{2ie^2(\Omega + 2i\Gamma)}{h}\Big[\frac{1}{(\Omega + 2i\Gamma)^2}\int_\Delta^\infty \frac{\omega^2 + \Delta^2}{\omega} \\ &\times \Big(\frac{\delta n_F(\omega)}{\delta\omega} - \frac{\delta n_F(-\omega)}{\delta\omega}\Big)d\omega \\ &- \int_\Delta^\infty \frac{\omega^2 + \Delta^2}{\omega}\Big(\frac{n_F(-\omega) - n_F(\omega)}{(\Omega + 2i\Gamma)^2 - 4\omega^2}\Big)d\omega\Big],\end{aligned} \tag{3}$$

where Ω is the optical frequency, $\Gamma = 7.6 \times 10^{12} s^{-1}$ is the scattering rate, $n_F(\omega)$ is the Fermi distribution function, ω is the energy of the relativistic Landau levels, and Δ is the exciton gap of Landau level energies. Assuming a finite thickness (d) of 0.7 nm of the graphene sheet, the relative permittivity of the graphene sheet can be calculated from the following equation,

$$\varepsilon_{eff} = 1 + i\frac{\sigma}{\Omega\varepsilon_0 d}, \tag{4}$$

where ε_0 is the relative permittivity of vacuum. Based on Eqs. (1)-(4), we calculated the relative permittivity of the graphene sheet with different initial Fermi levels and gas concentrations, as shown in Figure 1. The real part of the relative permittivity represents the phase change of light when interacting with graphene, while the imaginary part of the relative permittivity represents the optical loss induced by the graphene sheet. As shown in Figure 1(a), the real part of the relative permittivity decreases more rapidly at lower initial doping levels, so the incident light has a larger phase shift. Moreover, the variation of the imaginary part of the relative permittivity is relatively low for all the doping levels, since there is no interband transition in graphene when the Fermi level is beyond half of the photon energy (0.4 eV), as shown in Figure 1(b). Consequently, we chose the initial doping level of 0.41 eV in this work. Besides, the adsorbed gas molecules were strongly attached to the graphene devices at room temperature [16]. Graphene could be recovered to the undoped state by annealing at a high temperature, namely, from 323 K to 423 K in experiment [16], [28].

Finally, dual-mode resonance responses of the graphene-on-MRR to the gas concentration can be analyzed by using the transfer matrix method [29]. Different from single-mode MRRs, both TE_0 and TE_1 modes have phase changes (φ_0 and φ_1) with gas concentration (G) and temperature variation (T), which could be assumed as,

$$\begin{pmatrix}\varphi_0 \\ \varphi_1\end{pmatrix} = \begin{pmatrix}K_{0G} & K_{0T} \\ K_{1G} & K_{1T}\end{pmatrix}\begin{pmatrix}G \\ T\end{pmatrix}, \tag{5}$$

where K_{0G} and K_{1G} are the gas concentration sensitivities of the TE_0 and TE_1 modes, respectively, and K_{0T} and K_{1T}

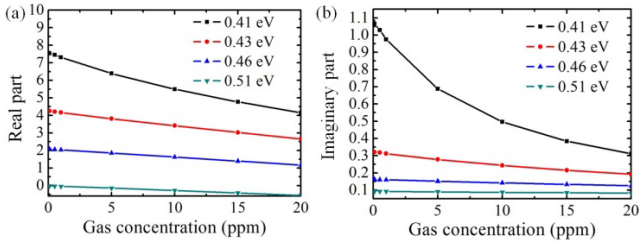

FIGURE 1. Calculated relative permittivity of graphene with different initial Fermi levels and gas doping concentrations. (a) Real parts of the relative permittivity as a function of gas concentration with different initial doping levels. (b) Imaginary parts of the relative permittivity as a function of gas concentration with different initial doping levels.

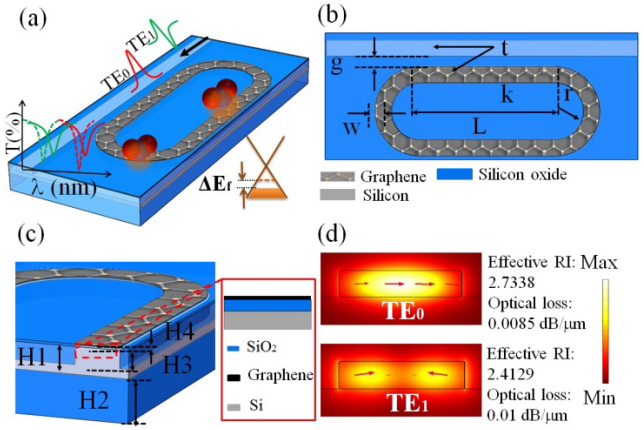

FIGURE 2. Schematics of the proposed optical gas sensor. (a) Three-dimensional view of the optical gas sensor. The gas-induced doping alternates the Fermi level of the graphene sheet, leading to the change of effective RIs of waveguide modes and shifts of resonant wavelengths. (b) Top view of the graphene-on-MRR. (c) Cross-section view of the proposed device. (d) Simulated electrical field distributions of TE_0 and TE_1 modes.

are the temperature sensitivities of the TE_0 and TE_1 modes. If the two modes have linearly independent responses to the variations of the gas concentration and temperature, the influences of these two factors can be decoupled by solving the following equation,

$$\begin{pmatrix} G \\ T \end{pmatrix} = \frac{1}{K_{0G}K_{1T} - K_{1G}K_{0T}} \begin{pmatrix} K_{1T} & -K_{0T} \\ -K_{1G} & K_{0G} \end{pmatrix} \begin{pmatrix} \varphi_0 \\ \varphi_1 \end{pmatrix}. \tag{6}$$

Phase signals φ_0 and φ_1 of the TE_0 and TE_1 modes, which are sensitive to the gas concentration and temperature variation, can be characterized by using a cavity, namely, MRR. As a result, we can separate graphene and temperature-induced RI variations in NO_2 molecular sensors based on the dual-mode graphene-on-MMR.

III. DESIGN AND SIMULATION RESULTS

Based on the above principle, we designed an optical gas sensor based on the graphene-on-MRR, as shown in Figure 2(a). A racetrack MRR was designed on a silicon-on-insulator wafer with a 220-nm thick top silicon layer (H1) and 3 μm buried oxide (BOX) (H2). As shown in Figure 2(b) and Figure 2(c), a waveguide width (W) was set as 1 μm with an etching depth (H3) of 200 nm, simultaneously supporting the TE_0 and TE_1 modes, while a bending radius (r) of the MRR was set as 20 μm introducing negligible radiation losses to the two modes. The waveguide is embedded in silicon oxide. A graphene sheet could be integrated on the surface of the MRR isolated by using a thin silicon oxide layer (H4). By adjusting the thickness of the isolation layer, it is possible to control the interaction strength between the propagating light and graphene sheet. In this work, we fixed the thickness of the isolation layer as 10 nm, which is feasible for experimental fabrication [30]. At the wavelength of 1550 nm and Fermi level of 0.41 eV, the effective RIs of the TE_0 and TE_1 modes were simulated as 2.7338 and 2.4129, respectively, by using a commercial finite element method (FEM) software tool (COMSOL Multiphysics). The optical loss coefficients are related to the imaginary parts of the complex effective RIs and are calculated as 0.0085 dB/μm and 0.01 dB/μm for the TE_0 and TE_1 modes, respectively. Figure 2(d) shows the simulated electrical field distributions of the two modes. Since the TE_0 and TE_1 modes have different effective RIs and optical losses, we need to properly design the coupling length (L) and gap width (g) of the MRR to satisfy the critical coupling conditions for the two modes.

The fabrication of the device is CMOS-compatible. The silicon devices can be fabricated by electron beam lithography (EBL) followed by dry etching. A thick silicon oxide layer could be deposited by using plasma-enhanced chemical vapor deposition (CVD). After that, the waveguide devices could be planarized by using chemical mechanical polishing to reach the top silicon layer. The commercial CVD graphene can be transferred onto the silicon device by using the standard wet transferring process. In the wet transfer process [17], the CVD graphene deposited on a copper foil could be first spin-coated with a layer of polymethyl methacrylate (PMMA). Then the copper foil could be etched away by using the ammonium persulfate solution. After rinsed in deionized water, the graphene supported by the PMMA layer could be transferred onto the silicon chip. The chip could be dried in the air and baked on a hot plate to allow better contact between graphene and waveguide devices. The EBL could be used to define the areas where the graphene layer should be exposed [17]. Then the O_2 plasma could be used to remove the exposed graphene areas. Finally, the remaining PMMA could be removed by acetone. The silicon waveguide could be used as a bottom gate to electrically tune the Fermi level of the graphene sheet.

Based on the proposed structure, we first numerically studied the dual-mode graphene-on-MRR. We simulated the cross-coupling power ratio (k^2) as a function of coupling length (L) under a fixed gap width (g) of 300 nm, as shown in Figure 3(a). With the L of 289.2 μm, the TE_0 and TE_1 modes have the same k of 0.4, which provides similar extinction ratios (ERs) for the two modes in the MRR. Moreover, we calculated the L needed to achieve the same k of the two modes for the different g, as presented in Figure 3(b).

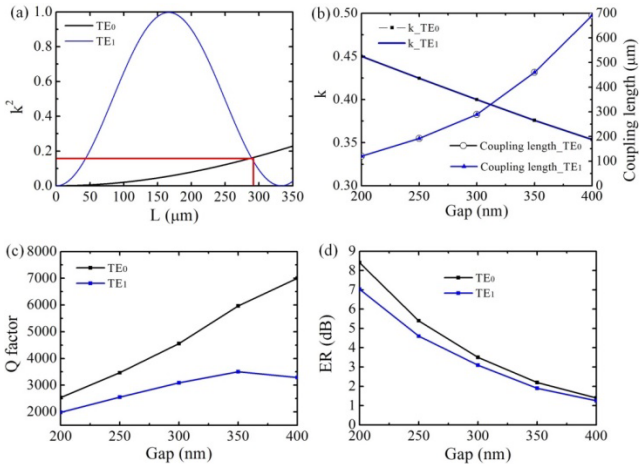

FIGURE 3. Design of the dual-mode graphene-on-MRR. (a) The cross-coupling optical power ratio (k^2) of the two modes as a function of coupling length (L) when the gap is 300 nm. (b) Cross-coupling coefficient (k) and coupling length needed to reach the same k for the two modes as a function of the coupling gap. (c) Q factors of the two modes as a function of the coupling gap. (d) ERs of the two modes as a function of the coupling gap.

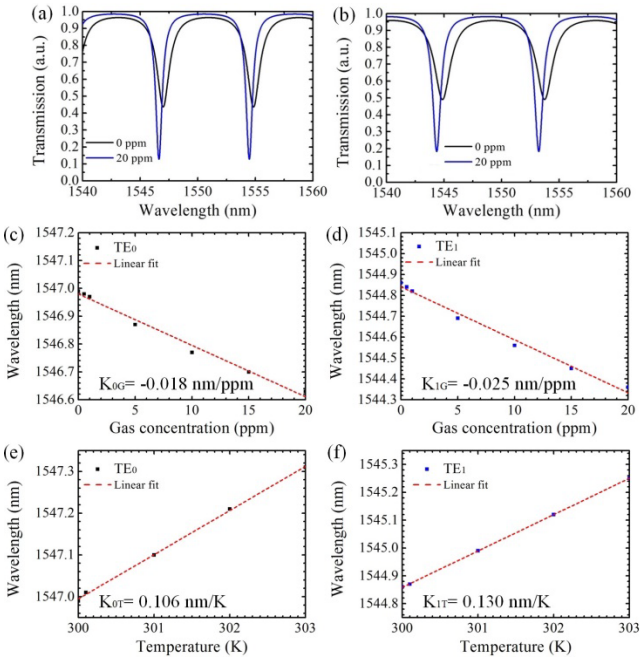

FIGURE 4. Optical properties of the proposed photonic gas sensor. (a) The transmission spectra for 0 ppm and 20 ppm NO_2 gaseous conditions of the TE_0 mode. (b) The transmission spectra for 0 ppm and 20 ppm NO_2 gaseous conditions of the TE_1 mode. (c) Resonance shift as a function of gas concentration for the TE_0 mode. (d) Resonance shift as a function of gas concentration for the TE_1 mode. (e) Resonance shift as a function of temperature for the TE_0 mode. (f) Resonance shift as a function of temperature for the TE_1 mode.

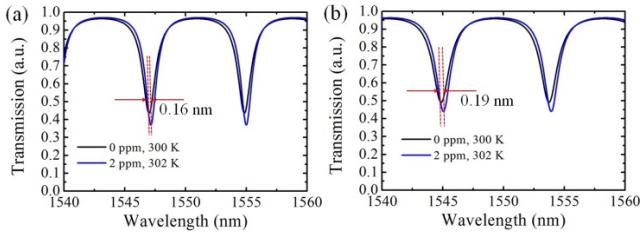

FIGURE 5. Transmission spectra of the two modes under the different conditions (NO_2 concentration of 0 ppm and 2 ppm, and temperatures of 300 K and 302 K). (a) Transmission spectra of the TE_0 mode. (b) Transmission spectra of the TE_1 mode.

Figure 3(b) indicates that with increasing the g, the L increases while the k decreases. Finally, we employed the above optical coefficients obtained to calculate quality (Q) factors [31] and ERs of the MRR, as shown in Figure 3(c) and Figure 3(d). By increasing the g, the Q factors quickly increase first and then become almost saturated. As RI sensors usually prefer a large Q factor, large ER, and small device footprint [32], we chose the g of 300 nm and L of 289.2 μm to develop the optical gas sensor.

Based on the designed dual-mode graphene-on-MRR device, we explored its application in NO_2 sensing under different temperatures. The shift of the resonance wavelength λ_{res} is essentially caused by a change of the effective RI of the resonant mode n_{eff} with $\Delta\lambda_{res} = \Delta n_{eff} L_{eff}/m$ [32], where L_{eff} is the effective length of the MRR, and m is the order of the mode. We first calculated the effective RIs, optical loss coefficients, and transmission spectra of the TE_0 and TE_1 modes with 0 ppm and 20 ppm NO_2 gas doping at a room temperature of 300 K, as shown in Figure 4(a) and Figure 4(b). When gas molecules are adsorbed on the graphene sheet, the Fermi level increases, leading to the decrease of effective RIs and optical losses, the resonant wavelengths, therefore, have blueshifts while the Q factors and ERs become larger. The resonant wavelengths of the two modes with different gas concentrations are shown in Figure 4(c) and Figure 4(d). The sensitivities from the linear fittings are -0.018 nm/ppm for the TE_0 mode (K_{0G}) and -0.025 nm/ppm for the TE_1 mode (K_{1G}), respectively. The LOD of the sensor is 0.5 ppm, which reaches the requirement of the Occupational Exposure Limit for NO_2 sensing in Europe (1ppm) [33]. By adjusting the waveguide geometry, the interactions between the waveguide modes and graphene can be tailored to modify the sensitivity and LOD. Then we calculated the temperature sensitivity of the sensor. In our model, we applied the thermo-optic coefficients of 1.8×10^{-4} /K of silicon [34] and 0.96×10^{-5} /K of silicon oxide [35] and simulated the effective RIs and optical loss coefficients of the two modes. The calculated resonant wavelengths at different temperatures are shown in Figure 4(e) and Figure 4(f). As the temperature increases, effective RIs of the two modes increase, leading to the redshifts of the resonant wavelengths. The temperature sensitivities are fitted as 0.106 nm/K for the TE_0 mode (K_{0T}) and 0.130 nm/K for the TE_1 mode (K_{1T}), respectively. The temperature sensitivities are four times larger than those of the gas concentration. Consequently, it is critical to eliminate the temperature variation when measuring the gas concentration by the RI sensing devices.

Finally, with the obtained gas concentration sensitivities ($K_{0G}$and K_{1G}) and temperature sensitivities ($K_{0T}$and K_{1T}) of the two modes, we demonstrated the optical gas sensor

TABLE 1. Comparision of our NO_2 sensor with previous works.

Sensor type	Senor structure	Sensitivity and LOD	Operation condition
On-chip optical sensor	Dual-mode graphene-on-MRR sensor in this work	Sensitivity of 0.02 nm/ppm and LOD of 0.5 ppm	Room temperature, 1550 nm wavelengths
Fiber optical sensor	Multimode optical fiber tip coated with a thin film of lutetium bisphthalocyanine[36]	Sensitivity of 5.02 mV/ppm (ratio of the photoresponse of photodiode connected to sensing fiber to the gas concentration), LOD of 1 ppm	Room temperature, 600 nm wavelengths
Metal oxide semiconductor sensor	Porous corundum-type In_2O_3 nanosheet gas sensor[37]	R_g/R_a (ratio of resistance in the test gas to the resistance in the air) response of 164 at 50 ppm gas concentration, LOD of 1 ppm	523 K operation temperature
Solid-electrolyte sensor	Solid-electrolyte sensor based on Yttria Stabilized Zirconia (YSZ) material[38]	Sensitivity of 0.5 mV/ppm (ratio of change of the potential between electrodes to gas concentration) in the gas concentration range of 20-100 ppm	723 K operation temperature

without suffering from the cross-sensitivity of temperature variations problem. Based on the above graphene-on-MRR design, the resonant wavelengths are 1546.99 nm for the TE_0 mode, and 1544.86 nm for the TE_1 mode, respectively, under a temperature of 300 K, as indicated by the black solid curves in Figure 5(a) and Figure 5(b). Then, we assumed a sensing condition with a gas concentration of 2 ppm and a temperature increase of 2 K. Based on Eqs. (1)-(4), the resonant wavelengths of the TE_0 and TE_1 modes shift to longer wavelengths by 0.16 nm and 0.19 nm, respectively. Based on the resonant wavelength shifts, we calculated gas concentration and temperature variations by using Eq. (6). The gas concentration and temperature increase were calculated as 2.1 ppm and 1.9 K, respectively, which are well consistent with the setting values. As a result, we theoretically demonstrated that the graphene-induced and temperature-induced RI variations could be decoupled by using the graphene-on-MMR. We compared the sensing performance of the proposed device with previous studies based on various approaches, such as the fiber-optic sensor [36], metal oxide semiconductor sensor [37], and solid-electrolyte gas sensor [38], as shown in Table 1. The LOD of the proposed device is comparable with those of the fiber-optic sensor and metal oxide semiconductor sensor but lower than that of the reported YSZ based solid-electrolyte gas sensor. It is worthwhile to know that the metal oxide semiconductor and solid-electrolyte gas sensors have to be operated at a high temperature. While the proposed device could work at room temperature and is not affected by the electromagnetic intervention.

IV. CONCLUSION

In summary, we theoretically studied the dual-mode graphene-on-MRR for gaseous NO_2 sensing. The device has a sensitivity of 0.02 nm/ppm and a LOD of 0.5 ppm. By using the dual-wavelength demodulation method, the gas concentration can be measured without suffering from temperature fluctuations. Our study is expected to boost the development of on-chip sensitive sensors with high temperature-stability for gas sensing.

REFERENCES

[1] J. Obermeier, P. Trefz, K. Wex, B. Sabel, J. K. Schubert, and W. Miekisch, "Electrochemical sensor system for breath analysis of aldehydes, CO and NO," *J. Breath Res.*, vol. 9, no. 1, Mar. 2015, Art. no. 016008.

[2] J. Huang, J. Zhou, Z. Liu, X. Li, Y. Geng, X. Tian, Y. Du, and Z. Qian, "Enhanced acetone-sensing properties to ppb detection level using Au/Pd-doped ZnO nanorod," *Sens. Actuators B, Chem.*, vol. 310, May 2020, Art. no. 127129.

[3] Z. Liu, J. Huang, Q. Wang, J. Zhou, J. Ye, X. Li, Y. Geng, Z. Liang, Y. Du, and X. Tian, "Indium oxide-black phosphorus composites for ultrasensitive nitrogen dioxide sensing at room temperature," *Sens. Actuators B, Chem.*, vol. 308, Apr. 2020, Art. no. 127650.

[4] H. Hokazono, W. Li, S. Enami, H. Jiang, and K. Hamamoto, "Gas sensing demonstration by using silica high-mesa waveguide with amplified cavity ring down spectroscopy technique," *IEICE Electron. Exp.*, vol. 12, no. 15, pp. 1–8, 2015.

[5] K. M. Yoo, J. Midkiff, A. Rostamian, C.-J. Chung, H. Dalir, and R. T. Chen, "InGaAs membrane waveguide: A promising platform for monolithic integrated mid-infrared optical gas sensor," *ACS Sensors*, vol. 5, no. 3, pp. 861–869, Mar. 2020.

[6] Q. Wang, Z. Wang, J. Chang, and W. Ren, "Fiber-ring laser-based intracavity photoacoustic spectroscopy for trace gas sensing," *Opt. Lett.*, vol. 42, no. 11, pp. 2114–2117, 2017.

[7] M. L. Notte, B. Troia, T. Muciaccia, C. Campanella, F. De Leonardis, and V. M. N. Passaro, "Recent advances in gas and chemical detection by Vernier effect-based photonic sensors," *Sensors*, vol. 14, no. 3, pp. 4831–4855, Mar. 2014.

[8] R. Yu, Y. Chen, L. Shui, and L. Xiao, "Hollow-core photonic crystal fiber gas sensing," *Sensors*, vol. 20, no. 10, pp. 1–27, 2020.

[9] Y. Lin, F. Liu, X. He, W. Jin, M. Zhang, F. Yang, H. L. Ho, Y. Tan, and L. Gu, "Distributed gas sensing with optical fibre photothermal interferometry," *Opt. Exp.*, vol. 25, no. 25, pp. 31568–31585, 2017.

[10] M. G. Manera and R. Rella, "Improved gas sensing performances in SPR sensors by transducers activation," *Sens. Actuators B, Chem.*, vol. 179, pp. 175–186, Mar. 2013.

[11] T. Lang, T. Hirsch, C. Fenzl, F. Brandl, and O. S. Wolfbeis, "Surface plasmon resonance sensor for dissolved and gaseous carbon dioxide," *Anal. Chem.*, vol. 84, no. 21, pp. 9085–9088, 2012.

[12] J. T. Robinson, L. Chen, and M. Lipson, "On-chip gas detection in silicon optical microcavities," *Opt. Exp.*, vol. 16, no. 6, pp. 4296–4301, Mar. 2008.

[13] P. Su, Z. Han, D. Kita, P. Becla, H. Lin, S. Deckoff-Jones, K. Richardson, L. C. Kimerling, J. Hu, and A. Agarwal, "Monolithic on-chip mid-IR methane gas sensor with waveguide-integrated detector," *Appl. Phys. Lett.*, vol. 114, no. 5, Feb. 2019, Art. no. 051103.
[14] W. R. Wong and P. Berini, "Integrated multichannel Young's interferometer sensor based on long-range surface plasmon waveguides," *Opt. Exp.*, vol. 27, no. 18, pp. 25470–25484, 2019.
[15] V. Mittal, N. P. Sessions, J. S. Wilkinson, and G. S. Murugan, "Optical quality ZnSe films and low loss waveguides on Si substrates for mid-infrared applications," *Opt. Mater. Exp.*, vol. 7, no. 3, pp. 712–725, 2017.
[16] F. Schedin, A. K. Geim, S. V. Morozov, E. W. Hill, P. Blake, M. I. Katsnelson, and K. S. Novoselov, "Detection of individual gas molecules adsorbed on graphene," *Nature Mater.*, vol. 6, no. 9, pp. 652–655, Sep. 2007.
[17] J. Wang, Z. Cheng, Z. Chen, X. Wan, B. Zhu, H. K. Tsang, C. Shu, and J. Xu, "High-responsivity graphene-on-silicon slot waveguide photodetectors," *Nanoscale*, vol. 8, no. 27, pp. 13206–13211, 2016.
[18] T.-H. Xiao, L. Gan, and Z.-Y. Li, "Efficient manipulation of graphene absorption by a simple dielectric cylinder," *Opt. Exp.*, vol. 23, no. 15, pp. 18975–18987, 2015.
[19] A. Maliakal, S. Husaini, L. Reith, P. Bollond, S. Cabot, P. Sheehan, S. Hangartar, S. Walton, and C. Tamanaha, "Graphene planar lightwave circuit sensors for chemical detection," *Proc. SPIE*, vol. 10107, Feb. 2017, Art. no. 101070T.
[20] Z. Cheng and K. Goda, "Design of waveguide-integrated graphene devices for photonic gas sensing," *Nanotechnology*, vol. 27, no. 50, Dec. 2016, Art. no. 505206.
[21] H. Kishikawa, M. Sato, N. Goto, S.-I. Yanagiya, T. Kaito, and S.-K. Liaw, "An optical ammonia gas sensor with adjustable sensitivity using a silicon microring resonator covered with monolayer graphene," *Jpn. J. Appl. Phys.*, vol. 58, Aug. 2019, Art. no. SJJD05.
[22] K. Li, J. Li, Y. Song, G. Fang, C. Li, Z. Feng, R. Su, B. Zeng, X. Wang, and C. Jin, "L_n slot photonic crystal microcavity for refractive index gas sensing," *IEEE Photon. J.*, vol. 6, no. 5, pp. 1–9, Oct. 2014.
[23] M. Singh, S. K. Raghuwanshi, and O. Prakash, "Modeling of grating assisted hybrid plasmonic filter and its on-chip gas sensing application," *IEEE Sensors J.*, vol. 19, no. 11, pp. 4039–4044, Jun. 2019.
[24] R. S. E. Shamy, M. A. Swillam, and D. A. Khalil, "Mid infrared integrated MZI gas sensor using suspended silicon waveguide," *J. Lightw. Technol.*, vol. 37, no. 17, pp. 4394–4400, Sep. 1, 2019.
[25] A. A. Abduljabar, N. Clark, J. Lees, and A. Porch, "Dual mode microwave microfluidic sensor for temperature variant liquid characterization," *IEEE Trans. Microw. Theory Techn.*, vol. 65, no. 7, pp. 2572–2582, Jul. 2017.
[26] N. Kazemi, M. Abdolrazzaghi, P. Musilek, and M. Daneshmand, "A temperature-compensated high-resolution microwave sensor using artificial neural network," *IEEE Microw. Wireless Compon. Lett.*, vol. 30, no. 9, pp. 919–922, Sep. 2020.
[27] V. P. Gusynin, S. G. Sharapov, and J. P. Carbotte, "Magneto-optical conductivity in graphene," *J. Phys., Condens. Matter*, vol. 19, no. 2, Jan. 2007, Art. no. 026222.
[28] S. Hwang, J. Lim, H. G. Park, W. K. Kim, D.-H. Kim, I. S. Song, J. H. Kim, S. Lee, D. H. Woo, and S. C. Jun, "Chemical vapor sensing properties of graphene based on geometrical evaluation," *Current Appl. Phys.*, vol. 12, no. 4, pp. 1017–1022, Jul. 2012.
[29] A. M. Vengsarkar, W. C. Michie, L. Jankovic, B. Culshaw, and R. O. Claus, "Fiber-optic dual-technique sensor for simultaneous measurement of strain and temperature," *J. Lightw. Technol.*, vol. 12, no. 1, pp. 170–177, Jan. 1994.
[30] X. Gan, R.-J. Shiue, Y. Gao, I. Meric, T. F. Heinz, K. Shepard, J. Hone, S. Assefa, and D. Englund, "Chip-integrated ultrafast graphene photodetector with high responsivity," *Nature Photon.*, vol. 7, no. 11, pp. 883–887, Nov. 2013.
[31] G. Yue, Z. Xing, H. Hu, Z. Cheng, G.-W. Lu, and T. Liu, "Graphene-based dual-mode modulators," *Opt. Exp.*, vol. 28, no. 12, pp. 18456–18471, 2020.
[32] W. Bogaerts, P. de Heyn, T. van Vaerenbergh, K. de Vos, S. K. Selvaraja, T. Claes, P. Dumon, P. Bienstman, D. van Thourhout, and R. Baets, "Silicon microring resonators," *Laser Photon. Rev.*, vol. 6, no. 1, pp. 47–73, 2012.
[33] *European Agency for Safety and Health at Work*. Accessed: Mar. 12, 2020. [Online]. Available: https://osha.europa.eu/en/legislation/directive/directive-2017164eu-indicative-occupational-exposure-limit-values
[34] J. Komma, C. Schwarz, G. Hofmann, D. Heinert, and R. Nawrodt, "Thermo-optic coefficient of silicon at 1550 nm and cryogenic temperatures," *Appl. Phys. Lett.*, vol. 101, no. 4, Jul. 2012, Art. no. 041905.
[35] A. W. Elshaari, I. E. Zadeh, K. D. Jöns, and V. Zwiller, "Thermo-optic characterization of silicon nitride resonators for cryogenic photonic circuits," *IEEE Photon. J.*, vol. 8, no. 3, Jun. 2016, Art. no. 2701009.
[36] A. Bueno, D. Lahem, C. Caucheteur, and M. Debliquy, "Reversible NO_2 optical fiber chemical sensor based on $LuPc_2$ using simultaneous transmission of UV and visible light," *Sensors*, vol. 15, no. 5, pp. 9870–9881, Apr. 2015.
[37] L. Gao, Z. Cheng, Q. Xiang, Y. Zhang, and J. Xu, "Porous corundum-type In_2O_3 nanosheets: Synthesis and NO_2 sensing properties," *Sens. Actuators B, Chem.*, vol. 208, pp. 436–443, Mar. 2015.
[38] I. Romanytsia, J.-P. Viricelle, P. Vernoux, and C. Pijolat, "Application of advanced morphology Au–X (X = YSZ, ZrO_2) composites as sensing electrode for solid state mixed-potential exhaust NO_x sensor," *Sens. Actuators B, Chem.*, vol. 207, pp. 391–397, Feb. 2015.

JIAQI WANG received the B.S. degree in optical information science and technology from the Huazhong University of Science and Technology, Wuhan, China, in 2012, and the Ph.D. degree in electronic engineering from The Chinese University of Hong Kong, Hong Kong, in 2016. She is currently an Assistant Professor with the College of Physics and Optoelectronic Engineering, Shenzhen University, Shenzhen, China. Her research interests include silicon photonics and fiber optic sensors.

XINYING ZHANG is currently pursuing the bachelor's degree with the College of Physics and Optoelectronic Engineering, Shenzhen University, Shenzhen, China. Her research interests include silicon photonics and graphene photonics.

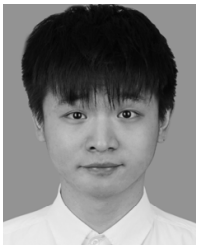

ZHIWEI WEI received the B.S. degree in optical information science and technology from Nanchang Hangkong University, China, in 2020. He is currently a Graduate Student with the College of Physics and Optoelectronic Engineering, Shenzhen University, Shenzhen, China. His research interests include silicon photonics and sensing properties of silicon-based waveguide devices.

HUABIN QIU received the B.S. degree in optical information science and technology from China Jiliang University, Hangzhou, China, in 2020. He is currently a Graduate Student with the College of Physics and Optoelectronic Engineering, Shenzhen University, Shenzhen, China. His research interests include silicon photonics and silicon waveguide integrated photodetectors.

YUZHI CHEN received the Ph.D. degree in physics from Shenzhen University, Shenzhen, China, in 2017. From 2017 to 2019, he was a Postdoctoral Fellow with The Chinese University of Hong Kong. He is currently an Assistant Professor with the College of Physics and Optoelectronic Engineering, Shenzhen University. His research interest includes fiber-optic sensors.

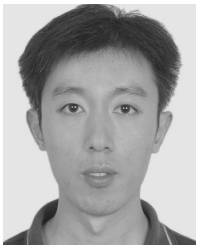

YOUFU GENG received the Ph.D. degree in physics from Tianjin University, Tianjin, China, in 2009. He is currently an Associate Professor with the College of Physics and Optoelectronic Engineering, Shenzhen University, Shenzhen, China. His research interest includes microstructured fiber optic sensors and devices.

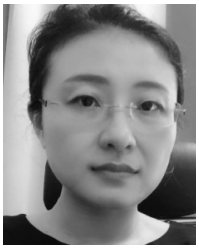

YU DU received the Ph.D. degree in chemistry from Jilin University, Jilin, China, in 2007. From 2007 to 2009, she was a Postdoctoral Fellow with Nanyang Technological University. She is currently a Professor with the College of Physics and Optoelectronic Engineering, Shenzhen University, Shenzhen, China. Her research interests include nanoscience and gas sensors.

ZHENZHOU CHENG (Senior Member, IEEE) received the B.S. degree in physics and the M.S. degree in optics from Nankai University, Tianjin, China, in 2006 and 2009, respectively, and the Ph.D. degree in electronic engineering from The Chinese University of Hong Kong, Hong Kong, in 2013. In 2015, he joined the Department of Chemistry, The University of Tokyo, Japan, as an Assistant Professor. In 2018, he joined the School of Precision Instruments and Optoelectronics Engineering, Tianjin University, Tianjin, as a Professor. His research interests include silicon photonics and graphene photonics for sensing, spectroscopy, nonlinear optics, and optical communications.

XUEJIN LI received the Ph.D. degree in physics from Tianjin University, Tianjin, China, in 2005. He is currently a Professor with the College of Physics and Optoelectronic Engineering, Shenzhen University, Shenzhen, China. His research interests include fiber-optic sensors and nonlinear optics.